Reverberation-based urban street sound level prediction

Pieter Thomas,[a)] Timothy Van Renterghem, Ellen De Boeck, Laurent Dragonetti, and Dick Botteldooren

Department of Information technology (INTEC),

Ghent University,

St. Pietersnieuwstraat 41,

B-9000 Gent,

Belgium

(Dated: January 5, 2014)

Abstract

Street reverberation can strongly increase sound pressure levels in urban streets. In noise mapping models on the other hand, including a sufficient number of reflections is computationally very costly. A simple regression model is developed in this study, based on typical street width and façade height or façade roughness in old city centers of many European cities. This model is based on measurements with a mobile setup in 99 streets in the city of Ghent, Belgium, representative for common European city morphology. The reflection ratio (RR) is used as a parameter to determine the energy contained in the reverberation part of the sound field. The model has been successfully validated by detailed measurements at different source-receiver distances in an urban street canyon.

PACS numbers: 43.50.Rq

I. INTRODUCTION

Sound propagation in urban street canyons is strongly influenced by multiple reflections in between building façades, leading to an important amplification of the sound relative to open terrain. This effect is important since the acoustic properties of the materials appearing in streets (concrete, bricks, windows, etc.) are close to acoustically rigid.

As a consequence, this leads to increased sound pressure levels, and to increased reverberation times[1,2]. Both aspects can be linked to an increased negative perception of noise. Street reverberation can be noticed especially for the case of a single passage of a motorized vehicle.

Realistic street geometries can be rather complex. It is expected that when streets are very wide, or the amount of open spaces in between buildings bordering the street is large, this enhancement will be much smaller. Furthermore, the effect of the finite length of streets, and the presence of cross-streets could potentially influence this reverberation gain. Also, scattering at building façade irregularities, building up diffuse sound fields in urban streets, is known to be an important aspect of urban street acoustics[3–8]. For narrow street canyons, interference effects play a significant role[9].

Noise maps are nowadays an important management tool for abating noise. However, producing urban noise maps comes at a high computational cost, mainly due to the large spatial extent one usually aims at. The use of simplified models, like e.g. ISO9613-2[10], does not relax this to a sufficient degree. As a practical, but inaccurate solution, the number of reflections is commonly reduced to only a few.

In this study, it is investigated to what extent the gain in sound pressure level due to the multiple reflections between building façades (and on the street surface) can be approached by simplified models, taking into account street dimensions and street characteristics only. The final goal, which is not the subject of this paper, is to use such a model to produce urban noise maps: only direct contributions from the source to the receiver points should then be

[a)] Electronic address: pieter.thomas@intec.ugent.be

considered, and the street amplification is added afterwards. The potential application of such a model is illustrated by means of a set of measurements performed in a real street.
A ray-tracing based approach has been used by Heutschi[11] to derive a simplified model of 'building correction' for a number of typical street geometries. Relevant parameters were the height of the façades, width of the street canyon (distance between the façades), the absorption coefficient of the façades, the degree of diffusion for reflections from the façades, and the source and receiver position. A correction was proposed for interrupted rows of buildings bordering a street. Here, a study with a similar purpose has been performed, which is now based on a large set of in-situ measurements in urban streets with a dedicated measurement setup. A model of similar complexity as in Heutschi's work is aimed at.
This paper is organized as follows. In section II, the measurement setup to determine the acoustical parameters in street canyons is described. The reflection ratio will be defined in section III: a prediction model for this parameter will be given, based on geometrical and architectural characteristics. With the reflection ratio, an estimate of the course of the sound pressure level along the length of a street canyon can be made. A description of the model and validation in a real street canyon is given in section IV.

II. MEASUREMENT SETUP

In order to be able to draw statistically relevant conclusions regarding the acoustical behavior of street canyons as a function of geometry, a vast amount of different streets needs to be investigated. This requires fast and easy impulse response measurements that do not disturb the traffic for too long. Therefore, the measurement setup was mounted on the roof of a car (Fig. 1). This setup contains an omnidirectional source with twelve speakers positioned on a dodecahedron. The source is mounted on the middle of the roof. Two free-field microphones of Bruël&Kjær, Type 4189, are placed at each side of the source, at a distance of $2.48\,m$. In this way, the measurement setup becomes very mobile, while two measurements can be done simultaneously to introduce a minimum of spatial averaging. It

further allows error detection, and investigating the influence of the body of the car on the measurements.

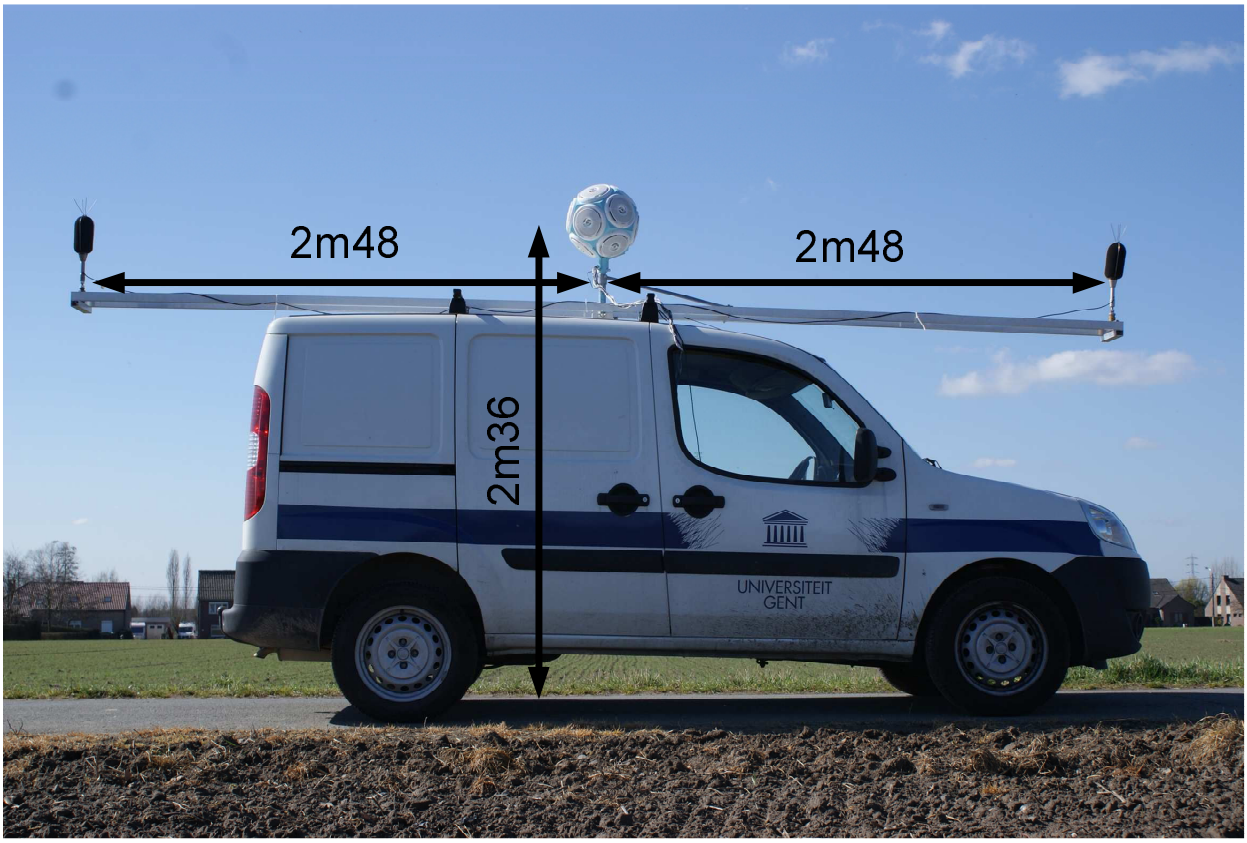

FIG. 1. Measurement setup with car for impulse response measurements. An omnidirectional source is placed on the middle of the roof. A free-field microphone (B&K Type 4189) is placed at 2.48 m at each side of the source.

A. Impulse response extraction

As measurements will take place in noisy outdoor environments, the choice of the excitation signal is critical. Therefore, a 30 s long exponential sweep with frequency span covering the 63 Hz to 16 kHz octave band was used. Since this type of signal excites only one frequency at a time, full sound power can be applied for each frequency, leading to improved signal to noise ratios compared to noise based techniques, where sound power is to be

distributed over all frequencies[12]. Furthermore, as the increase of frequency is exponential, each octave band contains an equal amount of energy. To increase the signal to noise ratio even more, the emission levels can be raised and averaging techniques can be applied.

The impulse response is calculated from the spectral division between the recorded and emitted sweep. In this paper we will focus on an octave band analysis of the parameters. For the octave band decomposition, a filter bank is used with 8th-order Butterworth octave band filters, following the ANSI S1.11-2004 standard[13].

As the band filtered impulse responses are likely to be contaminated with noise due to the outdoor environment, degenerating the quality of extracted parameters, start and endpoints need to be estimated[14]. The start point of the response is given by the time when the level-function of the impulse response, calculated by using the backwards integration technique[15], starts to decay. The endpoint or truncation point is estimated as the intersection between the decaying slope and averaged background noise level of the time-averaged squared band response[16].

B. Reflection ratio $RR(t_0)$

From the band filtered responses, several (room) acoustical parameters can be extracted. Also, in an urban environment, such parameters were shown to be useful to characterize the sound field[17,18]. In this work however we will focus on the reflection ratio $RR(t_0)$, a parameter which will prove to be useful for simplified noise map calculation:

$$RR(t_0) = 10 \log_{10} \left(\frac{\int_{t_0}^{\infty} h^2(\tau) d\tau}{\int_0^{t_0} h^2(\tau) d\tau} \right) \quad [dB] \tag{1}$$

The reflection ratio is the ratio of the sound energy of reflections arriving at the listener between time t_0 and $+\infty$ and the energy of the sound arriving from start to time t_0 and is extracted from the impulse response $h(t)$. The parameter is very useful when the sound intensity level of the direct sound or early sound field, $L_{early}(t_0)$, is known, since the level of the remaining part of the sound field (in [dB]) can be calculated as $L_{reflections} = RR(t_0) + L_{early}(t_0)$, with the dividing parameter t_0 indicating the span of the early sound field. Fig.

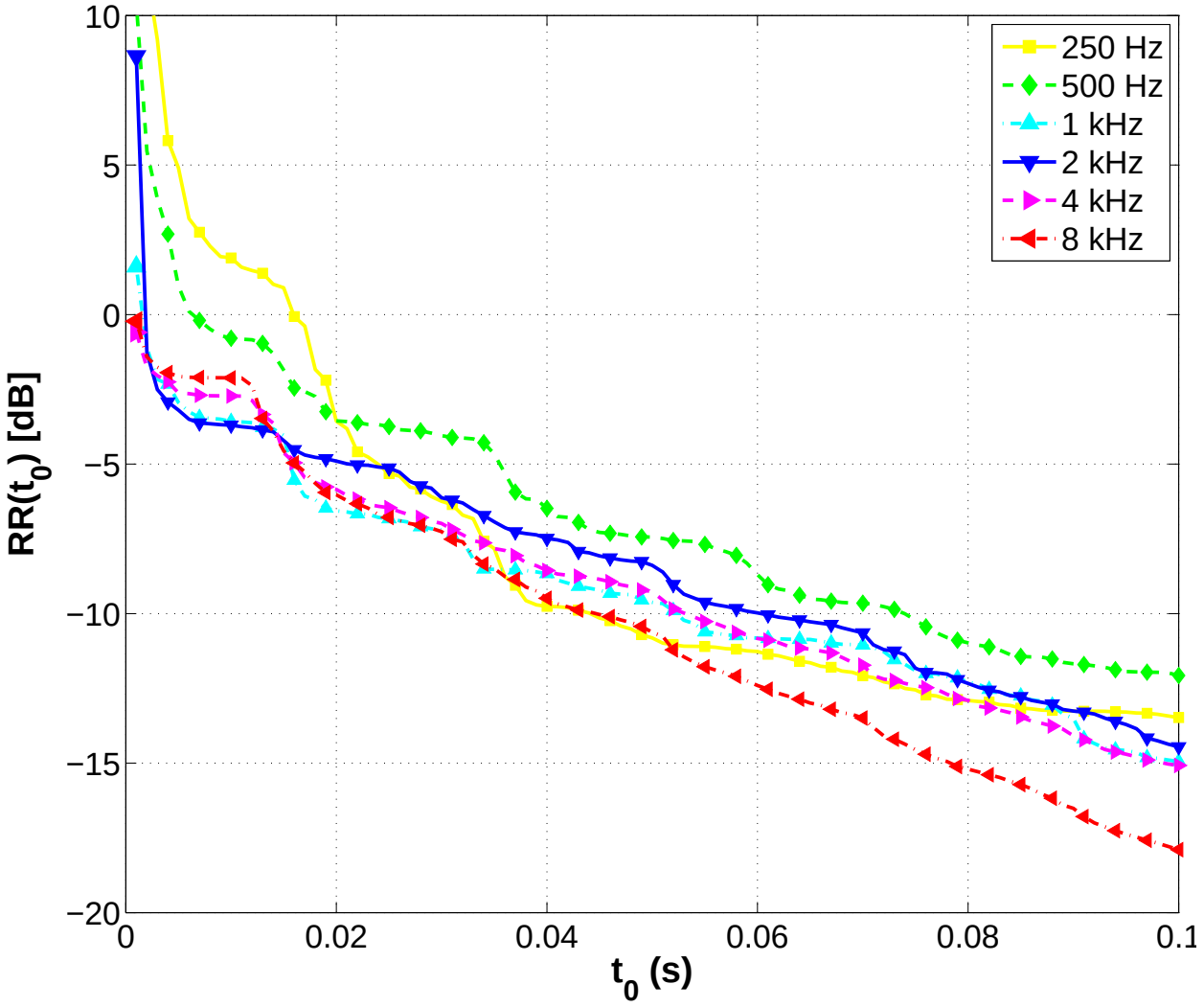

FIG. 2. Reflection ratio $RR(t_0)$ for the 250 Hz to 8 kHz octave band in a 5.4 m wide street. The arrival of early reflections, relative to the direct sound, can be noticed by sudden drops in the curve at multiples of the street width travel time (16 ms).

2 depicts the typical course of the reflection ratio in function of t_0 for the different octave bands in a 5.4 m wide street. The curve decays each time a reflection arrives at the listener, raising the energy in the denominator of $RR(t_0)$. In the early part of the reflection ratio, a stepwise decay is clearly visible, as the early sound field is built up out of discrete reflections from the façades. For higher t_0, the decay of $RR(t_0)$ is smoother as multiple reflections in the reverberant sound field arrive more continuously.

Assuming an image source model for geometrically reflecting façades[5], it can be deduced

that the steps of RR-decay are approximately located at multiples of the travel time between two opposing façades. For a simple model, with source and receiver at the same height in between two reflecting façades, the energy of the first reflection is given by:

$$E_{1\,st} = \frac{1-\alpha}{4\pi(w^2+\Delta_{ref}^2)} \tag{2}$$

with α the absorption coefficient of the façades, w the street width and Δ_{ref} the source-receiver distance. This expression can be generalized for the n^{th} reflection as:

$$E_{n\,th} = \frac{(1-\alpha)^n}{4\pi((nw)^2+\Delta_{ref}^2)} \tag{3}$$

The travel time needed for the n^{th} reflection to arrive at the receiver is given as $t_{n\,th} = c^{-1}\sqrt{(nw)^2+\Delta_{ref}^2}$, with c the speed of sound. The source receiver-distance Δ_{ref} in the measurement setup is (much) smaller than nw, so $t_{n\,th}$ can be approximated as $t_{n\,th} \approx c^{-1}nw$.

C. Validation in half-open space

All impulse response measurements and derived parameters are valid only if the influence of the measurement car is much lower than the influence of surroundings. In order to investigate this, impulse response measurements have been performed in an open rural area, without reflecting surfaces, except for the soil and the car itself. These reference measurements were conducted repeatedly at the start and the end of each measurement campaign in the city, in order to check the measurement setup. In total, 57 measurements in open field have been carried out over nine campaigns.

The average reflection ratio at the front end and rear end, together with the standard deviation, is plotted in Fig. 3 as a function of dividing time t_0. For the lowest octave band ($63\,Hz$), the standard deviation becomes too large ($\approx 5\,dB$ and even $> 7\,dB$ for $t_0 > 80\,ms$). This is due to the source, which is not suited to reproduce such low frequencies. Measurements at this octave band will not be taken into consideration.

For the other octave bands, the standard deviation for front and rear measurements remains limited to maximal $3.5\,dB$, even for high values of t_0. In general, both front and rear reflection ratios are alike and the small offset between front and rear (approx. $1.2\,dB$) remains

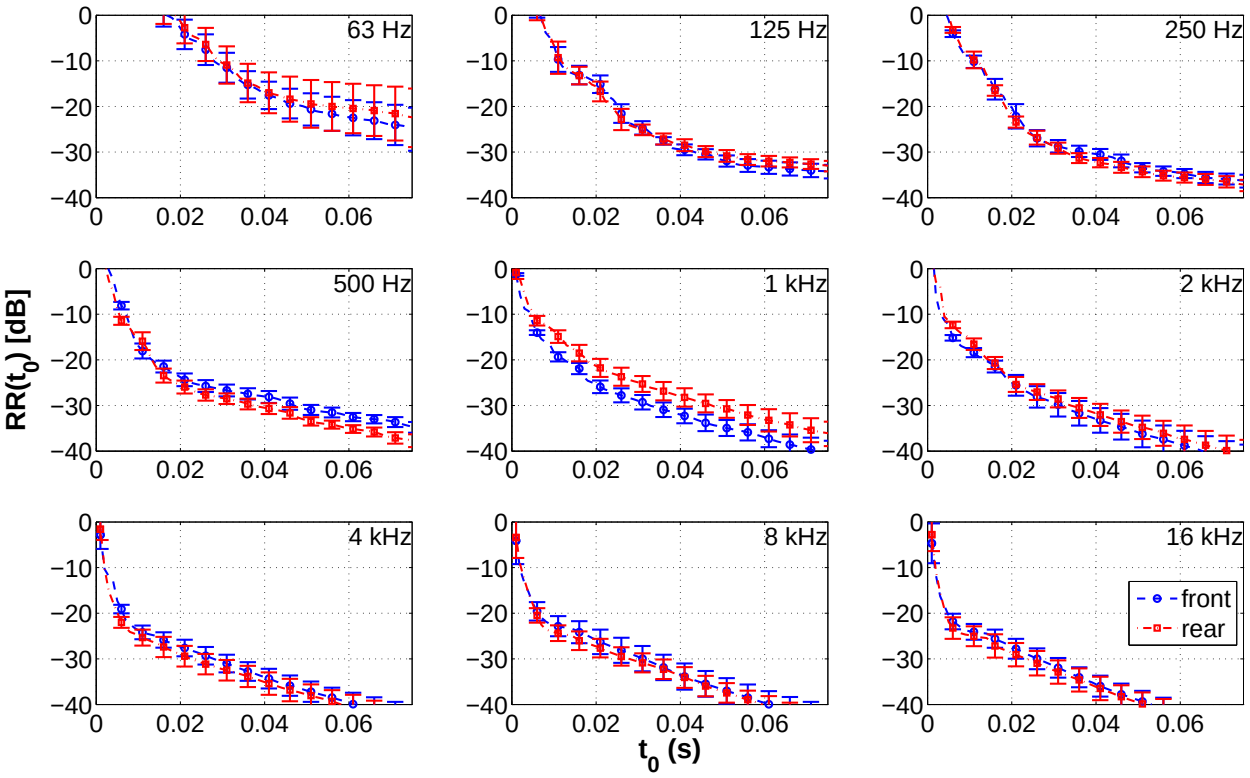

FIG. 3. Mean reflection ratio for 57 two-sided measurements in an open field, performed at different days. $RR(t_0)$ is depicted in function of the dividing time t_0 for the $63\,Hz$ - $16\,kHz$ octave band. Round markers ($\circ$) indicate the course of $RR(t_0)$ at the front end of the car and square markers ($\square$) indicate the course of $RR(t_0)$ at the rear end, with error bars indicating the standard deviation from the mean value.

within the standard deviation. However, for measurements in the $500\,Hz$ and $1\,kHz$ octave band, the difference between the average front and rear reflection ratio becomes higher ($2.2\,dB$ @ $500\,Hz$ and $4\,dB$ @ $1\,kHz$). It is concluded that the shape of the car has some (small) influence at the $1\,kHz$ (and $500\,Hz$) octave band. For further analysis this will not be accounted for and the averaged reflection ratio over front and rear reflection ratios will be used. Furthermore, as will be shown, the reflection ratio measured at the open field proves to be much lower than the different reflection ratios measured in urban streets. Thus, the influence of the car and measurement setup is small compared to the influence of the acoustics of urban streets and it is assumed that the measured reflection ratio is mainly

determined by the acoustics of the street.

III. STREET REFLECTION RATIO MEASUREMENTS

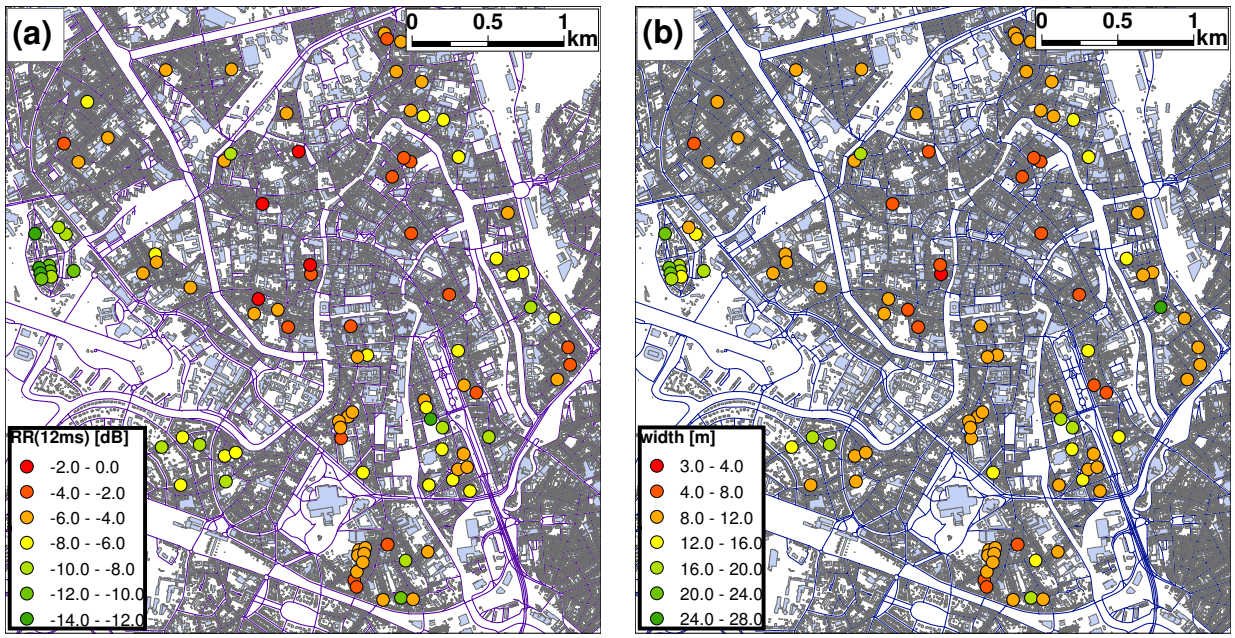

FIG. 4. Map indicating the location of the 99 measurement positions in the city of Ghent, Belgium. (a) Measured $RR(12\,ms)$ for the $1\,kHz$ octave band. (b) Street width at each measurement location.

Impulse responses at 99 different locations in the city of Ghent, Belgium, are measured, while different geometrical aspects of the location were noted. Where possible, the car is positioned in the center of the street. Measurements were repeated at least two times at each location, and averaged afterwards. Fig. 4 shows a map with the different locations where measurements were performed.

For the reflection ratio, $RR(t_0)$, the dividing time t_0 is chosen so that only the direct sound is contained in the denominator, while the energy of all reflections is contained in the numerator. In this way, the energy of the reflections can be derived from the energy of the direct sound. A dividing time t_0 of $12\,ms$ is chosen as a compromise between being able to measure $RR(t_0)$ in small streets and being able to ignore free field effects of the measure-

ment setup. The chosen t_0 corresponds to the travel time of the first reflection of a $4\,m$ wide street. Yet $RR(12\,ms)$ of the measurement setup remains lower than $-15\,dB$ for frequencies above $500\,Hz$.

A. Creating a model for $RR(12\,ms)$

In this section, a model based on different geometrical and architectural properties of the streets will be developed. The main geometrical characteristics include the street width (ranging between $3\,m$ and $25\,m$) and the average height of the façades (ranging between $5.5\,m$ and $15\,m$). In order to include the architectural properties, a visual categorization of the typical roughness of the street façades has been carried out. Initially, four categories were distinguished (Fig. 5). Streets with façades without regressions or protrusions relative to the façade plane (apart from where the windows and doors are located), are placed in a first category. The second category contains streets with façades with little relief and small ornaments, while in the third category streets with façades containing one balcony are classified. Streets where buildings have more than one bay window or balcony are classified in a fourth category. After location selection, large differences in category number count were noticed, so it was decided to keep category 1 (57 counts), renamed as category A, and combine category 2, 3 and 4 (42 counts) into category B. Although this is a rather crude approach, it allows studying whether including façade scattering increases correlation coefficients of the models.

1. Regression analysis based on street width

A very strong correlation between street width and reflection ratio was noticed. In order to maximize model fit, it is opted not to use the raw street width directly as input variable in a linear regression, but instead to use a simplified theoretical model for the reflection ratio ($RR_{1\,st}(w)$), assuming geometrically reflecting boundaries:

$$\widehat{RR}(12\,ms) = A \cdot RR_{1\,st}(w) + B \tag{4}$$

FIG. 5. Categorization of streets based on the typical roughness of the façades. Four categories are distinguished, ranging from flat façades to façades with many balconies and relief (a)-(d). For the final model, category 2 (b), 3 (c) and 4 (d) were merged to category B (dark frame), while category 1 (a) was renamed as category A.

For the simplified model of $RR_{1\,st}(w)$, only the direct sound and first reflections on both façades (given the measurement car is located in the center of the street) are taken into account:

$$RR_{1\,st}(w) = 10\log_{10}\frac{2/(4\,\pi\,(\Delta_{ref}^2 + w^2))}{1/(4\,\pi\,\Delta_{ref}^2)} \tag{5}$$

$$= 10\log_{10}\frac{2\Delta_{ref}^2}{\Delta_{ref}^2 + w^2} \tag{6}$$

with Δ_{ref} the distance between the source and receiver ($2.48\,m$) and w the street width.

Fig. 6 displays the measured $RR(12\,ms)$ for each street in function of $\log_{10}$(width). $RR(12\,ms)$, measured in the open field is indicated as well; the horizontal line gives the mean value, the horizontal dotted line is the standard deviation. In the $125\,Hz$ and $250\,Hz$ octave band, a small overlap between open field and street reflection ratio is seen only when streets are wider. On average however, $RR(12\,ms)$ of the open field remains lower than the measured street values. Starting from the $500\,Hz$ octave band, the overlap between street and open field measurements vanishes.

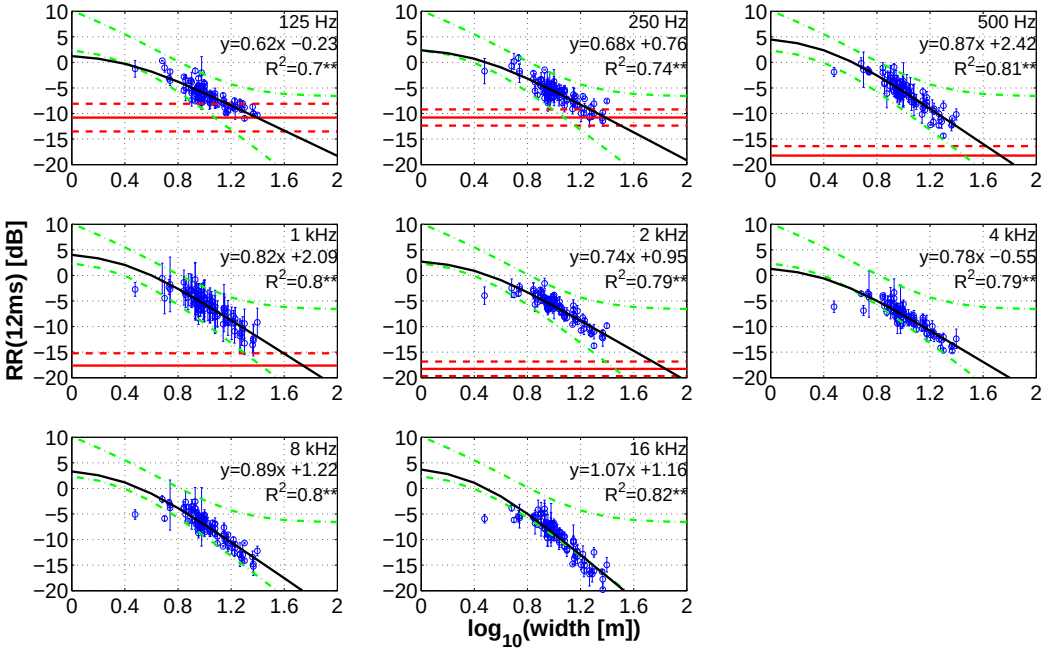

FIG. 6. Regression analysis of $RR(12\,ms)$ on 99 locations for different octave bands. The course of $\widehat{RR}(12\,ms) = A \cdot RR_{1\,st}(w) + B$ (full line) and its lower and upper bound (dashed-dotted line) is plotted in function of $\log_{10}(w)$. Measured $RR(12\,ms)$ is indicated by circles ($\circ$), with error bars indicating the standard deviation from the mean value at each location. $RR(12\,ms)$ of the open field is also indicated (mean value: horizontal line, mean value $\pm$ standard deviation: horizontal dashed line). The regression coefficients are indicated together with the squared correlation coefficient. * indicates $p < 0.05$, ** indicates $p < 0.01$.

The linear regression model shows strong correlation ($R^2 \approx 0.8$ on average) with the logarithm of the street width. For low and mid frequency bands, $RR_{1\,st}(w)$ itself is a lower bound for the measured reflection ratio: higher order reflections still have an important contribution. At high frequencies ($8\,kHz$ and $16\,kHz$) the simplified model is already sufficiently accurate in modeling the measured reflection ratio as higher order reflections are highly attenuated by air and façade absorption.

An upper bound for $RR(12\,ms)$ can be calculated based on the image source model for

geometrically reflecting boundaries. In order to calculate an upper limit RR_{max}, the energy contained in all reflections, including the ground reflections, needs to be summed. Eq. 3 describes the energy contained in the n^{th} reflection, calculated by only considering the street façades. In a similar way, the energy contained in the n^{th} ground reflection can be calculated as

$$E_{n\,th,gr} = \frac{(1-\alpha')(1-\alpha)^n}{4\pi((nw)^2 + 4H_{ref}^2 + \Delta_{ref}^2)} \tag{7}$$

with $H_{ref} = 2.36\,m$, the height of the source and receiver and α' the absorption coefficient of the ground surface. With Eq. 3 and Eq. 7, the upper bound can be modeled as

$$RR_{max} = 10\log_{10}\left(\frac{2\sum_{n=1}^{+\infty} E_{n\,th} + 2\sum_{n=1}^{+\infty} E_{n\,th,gr} + E_{0,gr}}{1/4\pi\Delta_{ref}^2}\right) \tag{8}$$

$$= 10\log_{10}\left(\frac{2\sum_{n=1}^{+\infty} \frac{(1-\alpha)^n}{4\pi((nw)^2+\Delta_{ref}^2)} + 2\sum_{n=1}^{+\infty} \frac{(1-\alpha')(1-\alpha)^n}{4\pi((nw)^2+4H_{ref}^2+\Delta_{ref}^2)} + (1-\alpha')/4\pi(\Delta_{ref}^2 + 4H_{ref}^2)}{1/4\pi\Delta_{ref}^2}\right) \tag{9}$$

If perfectly reflecting façades are assumed ($\alpha = \alpha' = 0$), this equation can be written as

$$\begin{aligned} RR_{max} = 10\log_{10}\Bigg(&\left(\frac{\pi\Delta_{ref}}{w}\coth\left(\frac{\pi\Delta_{ref}}{w}\right) - 1\right) \\ &+ \frac{\Delta_{ref}^2}{g_{ref}^2}\left(\frac{\pi g_{ref}}{w}\coth\left(\frac{\pi g_{ref}}{w}\right) - 1\right) + \frac{\Delta_{ref}^2}{g_{ref}^2}\Bigg) \end{aligned} \tag{10}$$

with $g_{ref}^2 = \Delta_{ref}^2 + 4H_{ref}^2$.

For low and mid frequency octave bands, RR_{max}, together with $RR_{1\,st}$ define a close interval to which $RR(12\,ms)$ is confined. For the high frequency octave bands, reflections are more attenuated by (air) absorption and RR_{max} becomes much higher than the measured values. Furthermore, it is seen that RR_{max} tends to saturate for increasing street width as the energy contained in the sums of Eq. 9 becomes smaller, relative to the energy contained in the direct sound and first ground reflection $E_{0,gr}$. In reality however, this first ground reflection will be less pronounced due to the presence of the car, but is included to show the upper limit.

2. Multiple regression analysis

In the previous section, only street width was used in the model. Although this model was already very satisfactory, this section will investigate if inclusion of other parameters (height of the street and façade roughness) can lead to further improvements.

Analysis of variance showed that height and façade roughness were not statistically independent (F-value 22.5, $p << 0.01$). This is not surprising, as in urban streets buildings are more likely to have more balconies (and higher degree of façade roughness) when building height increases. For this reason, both parameters cannot be used simultaneously as input variable in a multiple regression model. However, it is interesting to investigate the dependency of reflection ratio on building height and façade roughness. As both parameters are not necessarily known, it is decided to create two models, based on multiple regression analysis on the measured reflection ratio, with the simplified reflection ratio $RR_{1\,st}(w)$ (including street width) and one of both dependent parameters as input variables. Based on available data (either height or façade roughness), the appropriate model can then be selected.

In table I the resulting coefficients of the multiple regression analysis with $RR_{1\,st}(w)$ and the façade roughness as input parameters are displayed. Since the façade roughness is a categorical variable consisting of two categories, of which only one is statistically independent, this parameter is transformed into one independent dummy variable prior to inclusion in the model. The model then becomes

$$\widehat{RR}(12\,ms) = A \cdot RR_{1\,st}(w) + B \cdot roughnessCAT + C^{ste} \tag{11}$$

with $roughnessCAT = 1$ if the typical roughness of the façade is in category B and $roughnessCAT = 0$ in the other case.

At frequencies below the $1\,kHz$ octave band, façade roughness has no significant influence ($p > 0.05$). For higher frequencies, the positive contribution becomes statistically significant. Although small (max. $0.9\,dB$ @ $16\,kHz$), inclusion of the façade roughness leads

to some improvement, compared to the linear regression model solely based on $RR_{1\,st}(w)$. However, $RR_{1\,st}(w)$ remains the dominant factor over all octave bands: coefficients hardly differ compared to the previous regression model. The main reason for the small effect of façade roughness on the sound field in the streets is the presence of receivers very close to the source, which is a drawback of the employed measurement setup. By comparing the difference in SPL for a street canyon with geometrically reflecting façades (simulated by means of an image source method) with fully diffusely reflecting façades (simulated with the radiosity method), Kang[5] showed that diffuse reflections, caused by façade irregularities, indeed have an influence on the soundfield. For increasing source-receiver positions, an increase of attenuation was noted, whereas for positions close to the source, a small increase in SPL was seen due to backscattering effects. The tendencies found here are however statistically significant at frequencies where this is expected.

Table II gives the resulting coefficients from the multiple regression analysis for each octave band with $RR_{1\,st}(w)$ and the average height as input variables:

$$\widehat{RR}(12\,ms) = A \cdot RR_{1\,st}(w) + B \cdot (average\,height) + C^{ste} \tag{12}$$

This model has similar performance as the previous model. As average height and the categorization of façade roughness proved to be related, similar conclusions can be drawn. Starting from the $1\,kHz$ octave band, the contribution of the average height becomes significant ($p < 0.05$). At all octave bands, except at $125\,Hz$, the model implies that the average height has a positive influence on the reflection ratio. Indeed, increasing the height of the street enables more reflections to backscatter, raising $RR(12\,ms)$.

3. Model performance

This section describes the performance of the derived model by comparing the predicted reflection ratio with the measured reflection ratio. The model discussed here, is the one described in Table II, based on multiple regression analysis of $RR_{1\,st}(w)$ and the average

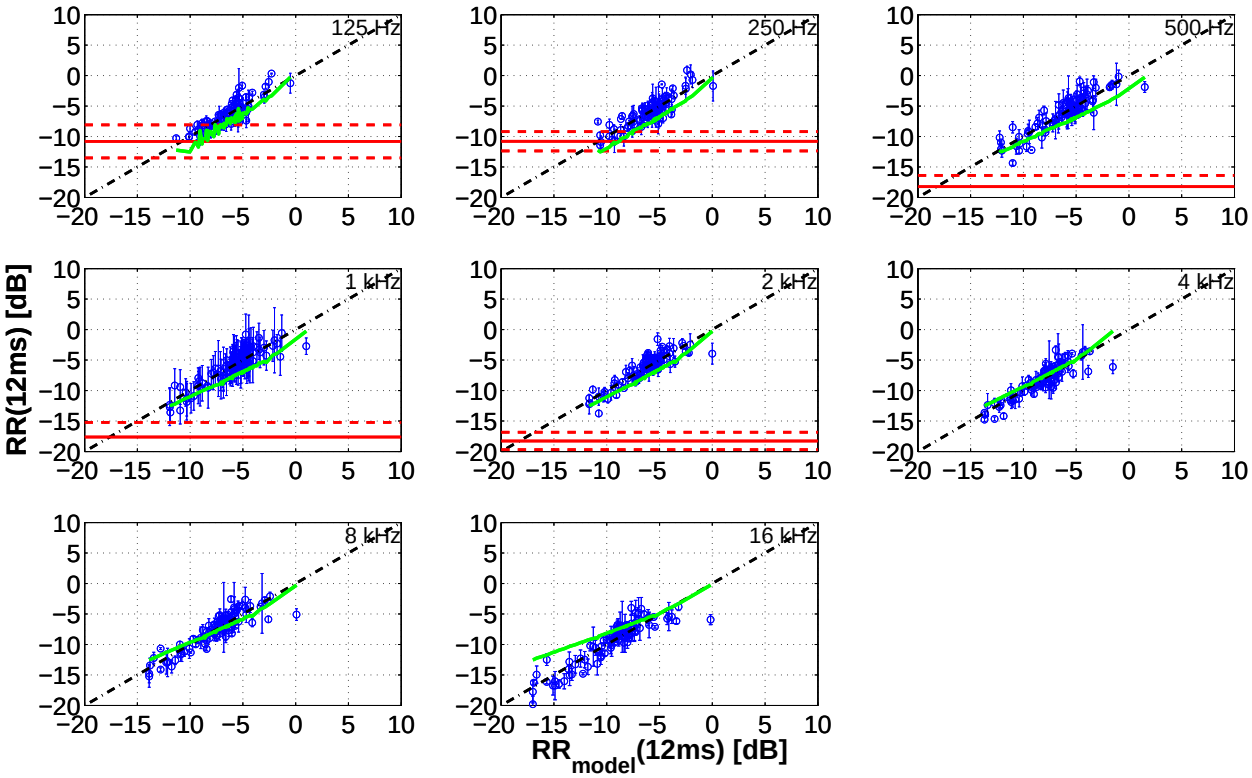

FIG. 7. Comparison between the predicted and measured reflection ratio. The x-coordinate gives the value of the modeled reflection ratio, based on the multiple regression model described in Table II. The corresponding measured reflection ratio is shown by discrete circles (∘), with error bars indicating the standard deviation from the mean value at each location. The full line shows the reflection ratio derived from Heutschi, plotted against the modeled reflection ratio based on the same geometrical data. The condition that should be met (1:1 mapping) is indicated by the dashed-dotted line. $RR(12\,ms)$ of the open field is also indicated (mean value: horizontal line, mean value ± standard deviation: horizontal dashed line).

height. This model is chosen as the average height is based on objective measurements, in contrast to the more subjective categorization of façade roughness. A comparison based on research from Heutschi[11] will also be made.

To incorporate the effect of the buildings, Heutschi defined the building correction BC_{SR} as the ratio of total energy to the energy of the direct sound for a given source-receiver position.

Based on extended ray tracing simulations, he derived a set of simple formulas, depending on the degree of diffusion, to estimate BC_{SR}. For general use however, a diffusion coefficient of $d = 0.2$ was proposed[11]. Under this condition, BC_{SR} is modeled as follows:

$$BC_{SR}|_{d=0.2} = \left(3.0 + 1.3 \log_{10}\left(\frac{h}{w}\right)\right) \frac{d_{SR}}{w} \quad [dB] \tag{13}$$

with h the façade height, w the street width and d_{SR} the source-receiver distance.
From BC_{SR} we can easily calculate the corresponding reflection ratio:

$$RR_{Heutschi} = 10 \log_{10}\left(10^{\frac{BC_{SR}}{10}} - 1\right) \quad [dB] \tag{14}$$

Fig. 7 depicts a comparison of the different models and the measured reflection ratio. The measured reflection ratio ($\circ$) at all 99 locations is plotted against the model based on $RR_{1\,st}(w)$ and average height at these locations. If the model is accurate, data should be on a straight line (1:1 mapping). Fig. 7 shows that this condition is fairly met. Only a limited part of the data points deviate from this line, but the highest deviation is less than $5\,dB$. When comparing the reflection ratio derived from Heutschi with the modeled reflection ratio, it is seen that $RR_{Heutschi}$ slightly underestimates ($\approx 2\,dB$) the modeled and measured reflection ratio for frequencies below the $2\,kHz$ octave band. In the $16\,kHz$ octave band, $RR_{Heutschi}$ delivers slightly higher prediction for the reflection ratio at low values. It should however be noted that the model based on $RR_{1\,st}(w)$ and average height incorporates frequency dependencies, while this is not the case in $RR_{Heutschi}$.

IV. PREDICTING SOUND PRESSURE LEVEL BASED ON THE REFLECTION RATIO.

In the previous section, a model for the reflection ratio has been created, based on an extensive measurement campaign. Here, it will be shown how the model can be used to predict sound pressure levels in a street canyon.

A. General model for the SPL in a street canyon

The energy of the direct sound (free field conditions) can be expressed as

$$E_{dir} \propto \frac{1}{4\pi r^2} \tag{15}$$

with r the source-receiver distance. Furthermore, in a street canyon, the reverberant energy can be approached by

$$E_{rev} \propto \frac{1}{2\pi r_{xz}} \tag{16}$$

with r_{xz} the projected source-receiver distance on the plane along the canyon, parallel with the façades. Propagation from a point source in between reflecting planes (here façades) can be considered as the geometrical divergence of a (badly discretized) line source. This corresponds to an energy decay of one over the distance at sufficient distances from the source.

Assuming that all distance dependence is captured by Eq. 15 and Eq. 16, the ratio of proportionality factors A_0 becomes distance independent, yet not frequency independent. A_0 can be related to $RR(12\,ms)$ by calculating the ratio of reverberant to direct field at the reference distance:

$$RR(12\,ms) = 10\,\log_{10}\frac{E_{rev}}{E_{dir}} \tag{17}$$

$$= 10\,\log_{10}\left(A_0\frac{1/(2\pi r_{xz})}{1/(4\pi r^2)}\right) \tag{18}$$

The reflection ratio at the reference source-receiver distance ($\Delta_{ref} = 2.48\,m$) can be estimated from the multiple regression model, based on the street width and average height. Given the reference source-receiver position along the canyon axis ($r = r_{xz} = \Delta_{ref}$) and $\widehat{RR}_{model}$, an estimate for A_0 can be extracted:

$$\widehat{A}_0 = \frac{10^{\frac{\widehat{RR}_{model}}{10}}}{2\Delta_{ref}} \tag{19}$$

With Eq. 19, the course of the total sound pressure level in a street canyon is calculated as

$$SPL \propto 10\,\log_{10}\left(E_{dir} + \widehat{A}_0\frac{b}{2\pi r_{xz}}\right) \quad [dB] \tag{20}$$

with E_{dir} the energy of the direct sound and b a correction factor, related to the source position relative to the ground. When the source is close to the ground, free field conditions are no longer valid, and an important ground reflection will be contained within the scope of the direct field ($t < 12\,ms$). This ground reflection is then not covered in the reverberant energy. Therefore, the direct energy, as defined by Eq. 15, will be extended with an additional ground reflection when the source is close to the ground. By using an image source for the ground reflection, the early soundfield can be calculated for each frequency as

$$p_{dir}(f) = \frac{1}{\sqrt{4\pi r^2}} e^{-\jmath k|r|} + \frac{1}{\sqrt{4\pi r'^2}} e^{-\jmath k|r'|} \tag{21}$$

with k the wave number, r the source-receiver distance and r' the distance between the mirrored source and receiver. E_{dir} is then calculated by summing the energy over the frequency bands: $E_{dir} = \sum_f |p_{early}(f)|^2$.

The proximity of the ground also influences the energy contained in the reverberant field. Therefore, a correction factor b is introduced, ranging between one (free field conditions) and two (source located at groundlevel and in case of a rigid street surface). A value in between one and two might be used in case of absorbing street surfaces.

B. Model validation in a real street canyon

In order to validate the proposed model, measurements of the sound pressure level in a real street canyon have been performed. Measurements in this street were not considered to build up the regression model. The selected street canyon is the 'Gustaaf Magnelstraat', a $105\,m$ long and $10.7\,m$ wide street. The average height is estimated at $17\,m$. The street was completely blocked for traffic during the measurements (Fig. 8). Only a few parked cars were present.

An omnidirectional source was positioned in the center of the street, $30\,cm$ above the asphalt, emitting a single $12\,s$ long exponential sweep. Receiver locations were chosen at multiples of $10\,m$ from the source, measured along the canyon axis, at $1.8\,m$ height. Two

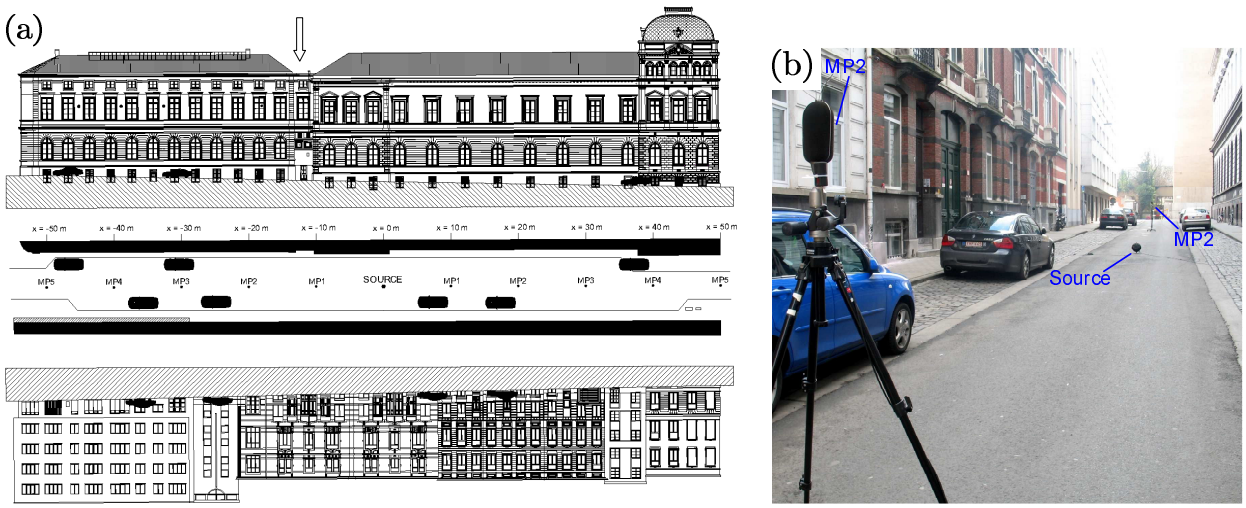

FIG. 8. Impulse response measurements in the 'Gustaaf Magnelstraat', a 105 m long and 10.7 m wide street canyon. The different measurement positions (MPx) along the canyon axis (x-axis) are indicated, as well as the source position (a). The arrow indicates the location of the façade depression. The center of the source was located 30 cm above the asphalt, the measurement microphones were at 1.8 m height (b).

MK250 omnidirectional microphones, one at each side of the source, were used to record the sweep signal. The resulting SPL at each position is extracted from the truncated impulse response, calculated as described in section II.A. At least four repeated measurements have been carried out at each location to enable averaging to further increase the signal-to-noise ratio.

Fig. 9 shows the course of the measured SPL along the street canyon axis together with the predicted SPL (Eq. 20, $b = 2$), based on $\widehat{RR}$ estimated with the simple model (Eq. 4), solely based on the street width, and the extended model (Eq. 12), including the average height. Here, a simple model for the atmospheric absorption has been included, based on ISO-9613[19] (measured meteorological parameters during the experiment: temperature = 5.0 $C°$, humidity = 80 % and atmospherical pressure = 997 hPa). As a reference, the averaged SPL at $x = -10\,m$ and $x = 10\,m$ is taken to be 0 dB for each model. The

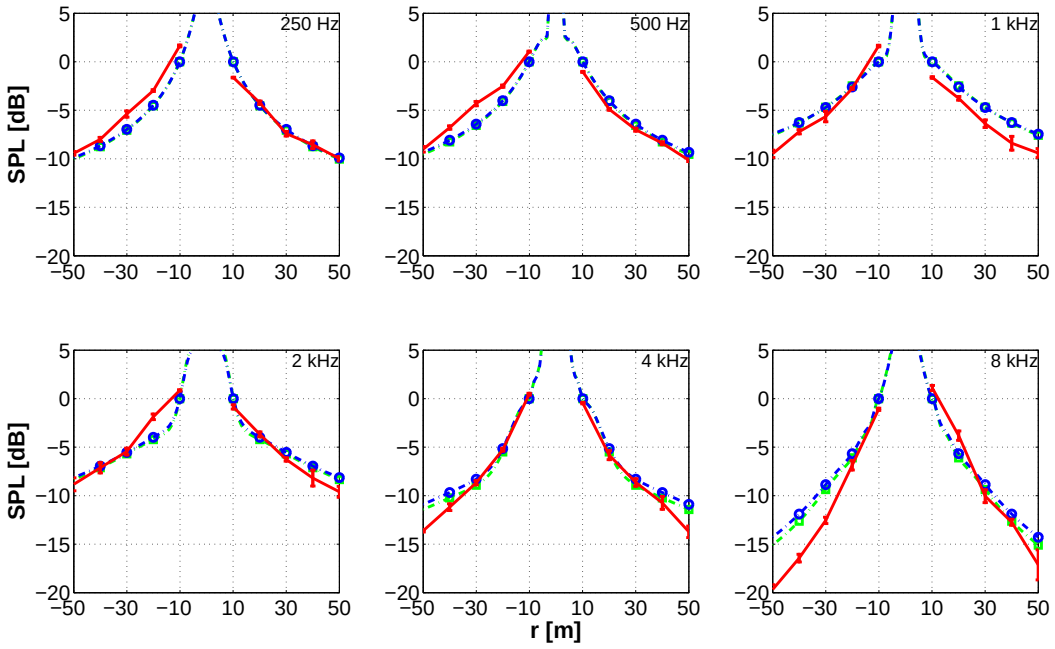

FIG. 9. Measurement and prediction of SPL in a street canyon in function of source-receiver distance for each octave band. The measured SPL is given, with error bars indicating the standard deviation from the mean value at each location. Square markers (□) indicate the SPL, modeled with the simple model for $\widehat{RR}$, solely based on the street width. Round markers (∘) indicate the SPL based on the extended model for $\widehat{RR}$, including the average height.

difference in course between the predicted SPL, based on the two different models for $\widehat{RR}$, is negligible after normalization. Only at the high frequency octave bands, a small difference ($< 1\,dB$) in SPL is seen. However, it must be noted that a frequency dependent offset exists between both SPL predictions (which is not seen due to the normalization), caused by a different estimate of $\widehat{RR}$. At low frequencies, these estimates differ approx. $0.3\,dB$, while at high frequencies a difference of approx. $1.5\,dB$ exists.

In contrast to the predicted SPL, the measured SPL has a non symmetrical course, with higher values for the left end of the street ($x \leq -10\,m$), that might be caused by some parked cars and a large façade depression near $x = -12\,m$ (Fig. 8). The larger density of

the cars parked at both sides of the left could virtually decrease the street width, giving rise to an increase of the measured SPL (see section IV.C). This effect is not seen at the $8\,kHz$ octave band, as the SPL is much lower than at the right end. For these high frequencies, the cars could act as large scattering objects, scattering part of the sound energy out of the street, consequently lowering the SPL. Differences up to $3.5\,dB$ were noted between positions left and right from the source at the same source-receiver distances.

Despite the asymmetric course of the measured sound pressure level, the predicted SPL still proves to be a good approximation. For the low and mid frequency octave bands, the differences between the predicted SPL and measured SPL are lower than $2\,dB$.

For the high frequency octave bands ($4\,kHz$ and $8\,kHz$), the measured SPL is slightly overpredicted near the ends of the street only.

C. Influence of street width and height on predicted SPL

This section investigates the dependency of the proposed SPL-model on the street width and average height. Based on Eq. 20, Eq. 19 and Eq. 12, the fluctuation of the total energy in function of street width can be calculated mathematically:

$$\frac{\partial\left(10\log_{10}\left(E_{dir}+\frac{b\widehat{A}_0}{2\pi r_{xz}}\right)\right)}{\partial w} = \frac{10}{\ln(10)}\frac{1}{E_{dir}+\frac{b\widehat{A}_0}{2\pi r_{xz}}}\frac{b}{2\pi r_{xz}}\frac{\partial\widehat{A}_0}{\partial w} \tag{22}$$

$$= \frac{\frac{b10^{RR/10}}{4\pi r_{xz}\Delta_{ref}}}{E_{dir}+\frac{b10^{RR/10}}{4\pi r_{xz}\Delta_{ref}}}\frac{\partial RR}{\partial w} \tag{23}$$

$$= -\frac{20A}{\ln(10)}\frac{1}{\frac{4\pi r_{xz}\Delta_{ref}E_{dir}}{b10^{RR/10}}+1}\frac{w}{\Delta_{ref}^2+w^2} \tag{24}$$

If we approximate the energy of the direct soundfield by $E_{dir}=\frac{b}{4\pi r^2}$ (no interference effects) and take $r=r_{xz}$ for source and receiver in the middle of the street, the derivative can be simplified to:

$$\frac{\partial SPL}{\partial w} = -\frac{20A}{\ln(10)}\frac{1}{\frac{\Delta_{ref}}{r_{xz}10^{RR/10}}+1}\frac{w}{\Delta_{ref}^2+w^2} \tag{25}$$

Since the coefficient A is always positive (Table II), Eq. 25 is always negative, which proves that the SPL is inversely proportional with the street width: increasing the width reduces the SPL. Furthermore, the change of total energy in function of width is bigger for changes relative to small street widths and positions further from the source as the magnitude of the derivative increases with decreasing street width and increasing distance r_{xz}.

In an analogue way, the variation of the SPL on the average height (H) can be calculated as well:

$$\frac{\partial\left(10\log_{10}\left(E_{dir}+\frac{b\widehat{A}_0}{2\pi r_{xz}}\right)\right)}{\partial H} = \frac{\frac{b10^{RR/10}}{4\pi r_{xz}\Delta_{ref}}}{E_{dir}+\frac{b10^{RR/10}}{4\pi r_{xz}\Delta_{ref}}}\frac{\partial RR}{\partial H} \tag{26}$$

$$= \frac{B}{\frac{4\pi r_{xz}\Delta_{ref}E_{dir}}{b10^{RR/10}}+1} \tag{27}$$

Again, E_{dir} is approximated by $E_{dir}=\frac{b}{4\pi r^2}$ and $r=r_{xz}$, simplifying the derivative:

$$\frac{\partial SPL}{\partial H} = \frac{B}{\frac{\Delta_{ref}}{r_{xz}10^{RR/10}}+1} \tag{28}$$

Eq. 28 proves that an increase of average height generally leads to an increase of SPL. For positions further from the source, the change of the SPL in function of the average height is bigger than for positions close to the source. The same conclusion can be drawn when changing the average height: relative to large heights, the change in SPL will be bigger than for low values (because of the factor $1/10^{RR/10}$ in the denominator). However, the effect of the average height on the derivative will be rather small, given the model coefficient $B<0.2$.

In order to give a more quantitative estimation of the influence of the width and average height on the predicted sound pressure level, a simulation is made for the source-receiver setup of the Magnelstraat with virtual street widths and heights. Fig. 10 shows the resulting course of the SPL, for street widths starting from $5\,m$ to $20\,m$ (full lines with triangular markers) and average heights starting from $5\,m$ to $20\,m$ (dashed lines with square markers). It is clear from the figure that the variation in SPL is much more dependent on variations of the street width than on variations of the average height. For low and mid frequency octave bands, changing the average height has almost no influence on the SPL (approx.

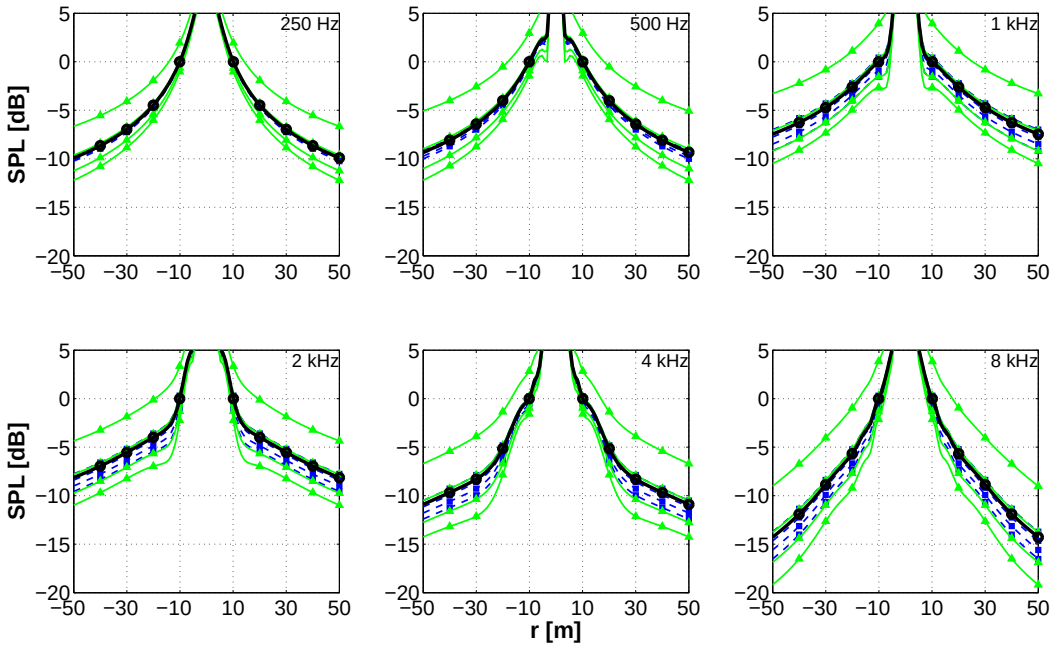

FIG. 10. Influence of the width and average height of the street canyon on the prediction of the SPL in function of the source-receiver distance for each octave band. The predicted SPL is given for the geometry of the Magnelstraat (width = $10.7\,m$ and average height = $17\,m$), plotted in full thick line with round markers (○). The full lines with triangular markers (▲) indicate the influence of the variation of street width on the SPL. The width is increased from $5\,m$ (uppermost curve) to $20\,m$ (lowest curve) in steps of $5\,m$. The dashed lines with square markers (■) show the variation of SPL in function of the average height. The height is varied in steps of $5\,m$ from $5\,m$ (lowest curve) to $20\,m$ (uppermost curve).

$2\,dB$ difference for the SPL at the $1\,kHz$ octave band between the extreme ranges of the average height at $x = 30\,m$). For higher frequency octave bands, the influence of the average height becomes somewhat higher (approx. $3.5\,dB$ difference at the $16\,kHz$ octave band). Changing the width however has a larger influence on the course of the SPL. Increasing the street width from $5\,m$ to $20\,m$ results in a decrease of $6.5\,dB$ at $x = 30\,m$ for the $1\,kHz$ octave band. This decrease is however not linearly proportional with the increase of street width, as a larger change in SPL is seen for changes at already low street width values.

Furthermore, it is seen from the figure that a change in street width has a bigger effect on the SPL for receiver positions further from the source. At $x = 30\,m$, the difference between the SPL at the extreme values the of street width is $6.5\,dB$, which increases to $7.2\,dB$ at $x = 50\,m$

V. CONCLUSION

In this paper, a new model is developed to predict sound pressure levels in urban streets. This model is based on the reflection ratio, defined as the reverberant to direct sound energy ratio. An extended measurement campaign has been set up to measure the reflection ratio in 99 streets in the city of Ghent, Belgium. A dedicated measurement setup has been designed, mounted on the roof of a car to enable fast and mobile measurements. The body of the car was shown to have negligible influence on this parameter. The latter has been assessed by measurements in the open field. The current measurement setup was able to quantify street reverberation starting at the octave band with center frequency of $125\,Hz$, at a sufficient repeatability.

Based on a few geometrical parameters such as street width, average height and façade roughness, a prediction model is proposed to estimate the reflection ratio. It is found that the reflection ratio highly correlates with the street width (i.e. the simplified reflection ratio $RR_{1\,st}(w)$) with $R^2 \approx 0.8$. Including the average street height or the building roughness slightly improves the proposed model. Resulting coefficients have been given and are tested with the real measured data and the model proposed by Heutschi. Good accordance is found.

To illustrate the use of the reflection ratio, a model for the total sound pressure level in a street canyon has been developed, where the ratio between direct sound energy and reverberant energy is extracted from the reflection ratio. The model has been verified with additional measurements in a city street canyon for different source-receiver positions. Although sound pressure measurements indicated that the distribution of sound energy was not symmetric

around the street center, the model was still able to roughly predict the course of the sound pressure levels, solely based on reflection ratio. Additionally, the influence of changes in the street width and average building height on the predicted SPL has been investigated.
In this work the potential of the reflection ratio to be used in urban noise map calculation has been illustrated. Once the direct sound energy contribution is known, the increase by street reverberation can be estimated. In this way calculation cost can be strongly reduced, without loss of accuracy. Furthermore, the reflection ratio can be easily predicted, based on simple geometrical street characteristics only.

References

[1] J. Kang, Urban sound environment (Taylor & Francis incorporating Spon, London) (2007), pp. 1–304.

[2] J. Picaut, T. L. Pollès, P. L'Hermite and V. Gary, "Experimental study of sound propagation in a street", Appl. Acoust. **66 (2)**, 149–173 (2005).

[3] R. Lyon, "Role of multiple reflections and reverberation in urban noise propagation", J. Acoust. Soc. Am. **55 (3)**, 493–503 (1974).

[4] J. Kang, "Numerical modelling of the sound fields in urban streets with diffusely reflecting boundaries", J. Sound Vib. **258**, 793–813 (2002).

[5] J. Kang, "Sound propagation in street canyons: Comparison between diffusely and geometrically reflecting boundaries", J. Acoust. Soc. Am. **107**, 1394–1404 (2000).

[6] J. Picaut, "Numerical modeling of urban sound fields by a diffusion process", Appl. Acoust. **63**, 965–991 (2002).

[7] T. Van Renterghem, E. Salomons and D. Botteldooren, "Parameter study of sound propagation between city canyons with coupled FDTD-PE model", Appl. Acoust. **67 (6)**, 487–510 (2006).

[8] M. R. Ismail and D. J. Oldham, "A scale model investigation of sound reflection from building façades", Appl. Acoust. **66**, 123–147 (2005).

[9] K. K. Iu and K. M. J. Li, "The propagation of sound in narrow street canyons", J. Acoust. Soc. Am. **112 (2)**, 537–550 (2002).

[10] ISO 9613-2:1996: "Acoustics - Attenuation of sound during propagation outdoors - Part 2: General method of calculation" (ISO, Switzerland, 1996).

[11] K. Heutschi, "A simple method to evaluate the increase of traffic noise emission level due to buildings, for a long straight street", Appl. Acoust. **44**, 259–274 (1995).

[12] ISO 18233:2006(E): "Acoustics - Application of new measurement method in building and room acoustics" (ISO, Switzerland, 2006).

[13] ANSI S1.11-2004: "Specification for octave-band and fractional-octave-band analog and digital filters" (ANSI, New York, 2009).

[14] P. Thomas, T. Van Renterghem and D. Botteldooren, "Using room acoustical parameters for evaluating the quality of urban squares for open-air rock concerts", Appl. Acoust. **72**, 210–220 (2011).

[15] M. Schroeder, "New method of measuring reverberation time", J. Acoust. Soc. Am. **37**, 409–412 (1965).

[16] A. Lundeby, T. Vigran, H. Bietz and M. Vorländer, "Uncertainties of measurements in room acoustics", Acustica **81**, 344–355 (1995).

[17] E. Schröder, "Nachhall in geschlossenen bebauten strassen" ("Reverberation in closed urban streets"), Lärmbekämpfung **17**, 11–18 (1973).

[18] P. Thomas, E. De Boeck, L. Dragonetti, T. Van Renterghem and D. Botteldooren, "Creating an urban street reverberation map", Proc. of Forum Acusticum 397–402 (2011).

[19] ISO 9613-1:1993: "Acoustics - Attenuation of sound during propagation outdoors - Part 1: Calculation of the absorption of sound by the atmosphere" (ISO, Switzerland, 1993).

TABLE I. Results of the multiple regression analysis on the measured reflection ratio, with $RR_{1\,st}(w)$ and the façade roughness as input variables. The squared correlation coefficient of the model is also given (* indicates $p < 0.05$, ** indicates $p < 0.01$).

	Model coefficients			
f_{oct}	C^{ste}	$RR_{1\,st}(w)$	roughness CAT	R^2
$125\,Hz$	-0.111	0.615^{**}	-0.429	0.71^{**}
$250\,Hz$	0.673	0.688^{**}	0.295	0.74^{**}
$500\,Hz$	2.327^{**}	0.876^{**}	0.346	0.81^{**}
$1\,kHz$	1.933^{**}	0.831^{**}	0.550^{*}	0.81^{**}
$2\,kHz$	0.828^{*}	0.749^{**}	0.418	0.80^{**}
$4\,kHz$	-0.726	0.784^{**}	0.619^{*}	0.80^{**}
$8\,kHz$	0.986^{*}	0.901^{**}	0.840^{**}	0.82^{**}
$16\,kHz$	0.915	1.086^{**}	0.865^{**}	0.83^{**}

TABLE II. Results of the multiple regression analysis on the measured reflection ratio, with $RR_{1\,st}(w)$ and the average height as input variables. The squared correlation coefficient of the model is also given (* indicates $p < 0.05$, ** indicates $p < 0.01$).

	Model coefficients			
f_{oct}	C^{ste}	$RR_{1\,st}(w)$	Average height	R^2
$125\,Hz$	1.209	0.627^{**}	-0.164^{**}	0.72^{**}
$250\,Hz$	0.420	0.683^{**}	0.038	0.74^{**}
$500\,Hz$	1.741^{*}	0.868^{**}	0.078	0.81^{**}
$1\,kHz$	0.414	0.816^{**}	0.190^{**}	0.82^{**}
$2\,kHz$	-0.412	0.737^{**}	0.154^{**}	0.80^{**}
$4\,kHz$	-1.864^{**}	0.770^{**}	0.149^{*}	0.80^{**}
$8\,kHz$	-0.442	0.882^{**}	0.189^{**}	0.81^{**}
$16\,kHz$	-0.576	1.066^{**}	0.197^{*}	0.83^{**}

List of Figures